Optics Letters

Femtosecond laser line-by-line tilted Bragg grating inscription in single-mode step-index TOPAS/ZEONEX polymer optical fiber

Hang Qu,[1] Zhen Chen,[1] Shixin Gao,[2] Rui Min,[3] Getinet Woyessa,[4] Ole Bang,[4] Heng Wang,[2] Christophe Caucheteur,[5] and Xuehao Hu[5,*]

[1]Research Center for Advanced Optics and Photoelectronics, Department of Physics, College of Science, Shantou University, Shantou, Guangdong 515063, China
[2]College of Science, Shenyang Aerospace University, Shenyang 110136, China
[3]Center for Cognition and Neuroergonomics, State Key Laboratory of Cognitive Neuroscience and Learning, Beijing Normal University, Zhuhai, Guangdong 519087, China
[4]DTU Electro, Department of Electrical and Photonics Engineering, Technical University of Denmark, 2800 Kgs. Lyngby, Denmark
[5]Department of Electromagnetism and Telecommunication, University of Mons, Boulevard Dolez 31, 7000 Mons, Belgium
*Corresponding author: xuehao.hu@umons.ac.be

Received 1 December 2022; revised 12 January 2023; accepted 6 February 2023; posted 6 February 2023; published 7 March 2023

In this Letter, we demonstrate 8°-tilted fiber Bragg grating (TFBG) inscription in single-mode step-index TOPAS/ZEONEX polymer optical fibers (POFs) using a 520 nm femtosecond laser and the line-by-line (LbL) writing technique. As a result of the tilt angle and the fiber refractive index, a large spectral range of cladding mode resonances covering 147 nm is obtained. The evolution of the transmitted spectrum is analyzed as a function of the surrounding refractive index (SRI) in a large range from 1.30 to 1.50. The cutoff cladding mode shows a refractive index sensitivity of 507 nm/RIU (refractive index unit). For single-resonance tracking near the cutoff mode, the sensitivity is at least 6 nm/RIU, depending on the exact wavelength position of the cladding modes. The main originality of our work is that it produces, for the first time, to the best of our knowledge, a TFBG in POF that operates in the refractive index range of aqueous solutions. The sensing capability for a large range of refractive index values is also relevant for (bio)chemical sensing in different media.

https://doi.org/10.1364/OL.482598

Fiber Bragg gratings (FBGs) in polymer optical fibers (POFs) have been developed in various materials, such as poly(methyl methacrylate) (PMMA) [1–3], cyclic olefin copolymers (TOPAS) [4–6], cyclic transparent amorphous fluoropolymers (CYTOP) [7], a cyclic olefin polymer (ZEONEX) [8,9], and polycarbonate (PC) [10]. Due to the unique advantages of polymer optical fibers (POFs) compared to their silica counterparts, such as larger thermo-optic coefficients, smaller Young's moduli, and good biocompatibility, uniform FBGs in POFs have mainly been used in physical applications, including for measurements of temperature, strain, or humidity [7,11].

Regarding grating inscription in POFs, phase mask lithography has naturally been the most popular and frequently used technique to date. In 2002, Liu *et al.* manufactured a highly reflective grating (reflectivity: ~99.8%) in a PMMA-based POF using a 325 nm laser [12]. In 2018, Pereira *et al.* inscribed an FBG in benzyl dimethyl ketal (BDK)-doped PMMA mPOFs [13] with a reflectivity of 84% using a single laser pulse at 266 nm [14]. In addition to the phase mask technique, tightly focused femtosecond laser pulses have also been reported for manufacturing FBGs in POFs. Theodosiou and Kalli succeeded in inscribing an FBG into CYTOP fiber using the femtosecond laser plane-by-plane (Pl-b-Pl) technique [15]. In 2022, our group also reported the fabrication of a first-order FBG in BDK-doped step-index PMMA POFs using the femtosecond laser point-by-point (PbP) technique and achieved a high reflectivity of 98.8% [16].

Tilted fiber Bragg gratings (TFBGs) have a similar grating period to FBGs but with a refractive index modulation that is slightly angled with respect to the direction perpendicular to the optical fiber propagation axis. Two kinds of couplings emerge, i.e., the self-backward coupling of the core mode and multiple backward couplings between the core mode and cladding modes [17]. TFBGs nominally feature several tens of narrowband cladding mode resonances in their transmitted amplitude spectra. These resonances can be directly used for applications involving the sensing of the surrounding refractive index (SRI) [18] without the requirement for fiber de-cladding or tapering to create a light–matter overlap. TFBG-based sensors can inherently provide temperature compensation, as the core mode is responsive to temperature perturbations but not to SRI variations.

Similarly to the fabrication of FBGs in silica fibers, TFBGs are inscribed either by interference between two UV laser beams [19] or by femtosecond laser direct writing [20]. Important progress has been obtained over the past decade, and relevant examples will be highlighted hereafter. In 2003, Zhou *et al.* inscribed TFBGs with tilt angles of up to 18° in silica fibers by both phase-mask and holographic techniques [21]. In 2016, a

16-mm-long 37° TFBG photo-inscribed in a single-mode silica fiber with a uniform phase mask was reported. Cladding modes with effective indices of ~1.0 were obtained [22]. In 2018, Ioannou *et al.* fabricated higher-order TFBGs in a single-mode silica fiber by the femtosecond laser Pl-b-Pl technique [23]. In 2022, the inscription of TFBG in boron-co-doped fibers using a low-cost 266 nm solid state pulsed laser and the scanning phase mask technique was achieved [24].

Though TFBGs in silica fibers are well developed, TFBG fabrications in POFs have only been reported in our previous works [25,26]. In 2014, we inscribed the first TFBGs in *trans*-4-stilbenemethanol-doped photosensitive step-index PMMA POFs with tilt angles of up to 4.5° using a He-Cd laser emitting at 325 nm and the phase mask technique [25]. The following year, the tilt angle for the TFBGs was increased to 6° using the same fiber and experimental setup. Based on this sample, surface plasmon resonance was first reported in POF-based TFBGs surrounded by a thin gold film [26]. Due to small tilt angles and the high refractive index of PMMA, these refractometric sensors could only be applied to monitor SRIs higher than 1.4 RIU (refractive index unit), which is far from the target index (~1.33) of aqueous solutions usually used for biochemical sensing. However, it is difficult to efficiently fabricate TFBGs with higher tilt angles (for instance up to 10°) for lower refractive index monitoring. This issue arises from the decrease in the coupling efficiency with higher tilt angles [27] and the inherent properties of the polymer, such as higher absorption of UV light and higher thermal swelling due to laser heating compared to silica fibers.

Motivated by the desire to produce TFBGs with a higher tilt angle that can be effectively used in standard aqueous solutions, we report the first—to the best of our knowledge—TFBG photo-inscription in single-mode step-index TOPAS/ZEONEX POFs by the line-by-line (LbL) technique with a 520 nm femtosecond laser. As both TOPAS and ZEONEX have glass transition temperatures above 130°C [28], which are higher than that of PMMA (108°C) [29], the TOPAS/ZEONEX POFs are less influenced by heat than the PMMA POFs. Compared to other laser writing techniques, femtosecond direct writing technology presents the unique advantages of high accuracy and quality with a reduced thermal effect [30]. In our previous work, we reported the fabrication of standard FBG in the same type of POF via the PbP technique [31]. However, this technique cannot be adopted for TFBG inscription. Therefore, we rely on the LbL inscription method for TFBG fabrication. The POF features a core material of TOPAS (5013S-04, TOPAS Advanced Polymers) with an index of 1.5238 (@850 nm) and a cladding material of ZEONEX (480R, Zeon Corporation) with an index of 1.5179 (@850 nm). The POF used in this work was fabricated in-house at DTU Electro with a core diameter of 5 μm and a cladding diameter of 128 μm [28]. Unlike PMMA, which features a high water affinity of up to 2% [32], these two materials have water absorption rates of under 0.01% [10] and thus are less sensitive to moisture interference when performing SRI measurements.

In this work, 8° TFBGs were produced, and their transmitted amplitude spectrum contains cladding mode resonances covering a large spectral range of 147 nm. The evolution of the transmitted spectrum is monitored as a function of SRI in the range from 1.30 to 1.50. Tracking the wavelength shift of the cutoff cladding mode yields a sensitivity of 507 nm/RIU. This work shows a breakthrough for TFBG fabrication in POFs, as it provides effective operation in the refractive index range of aqueous solutions. In addition, the sensing capability for a large range of SRI values is quite favorable for (bio)chemical sensing in different media.

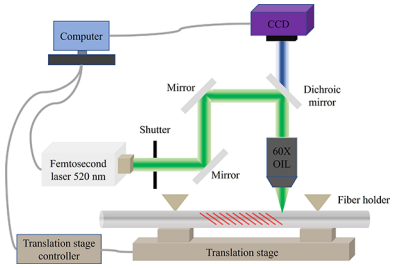

Fig. 1. Illustration of the setup for LbL TFBG inscription.

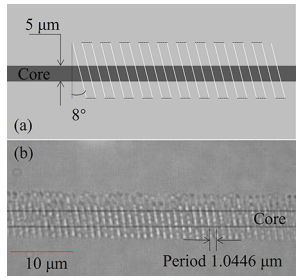

Fig. 2. (a) Schematic of the laser-scanning process; (b) microscopic image of TFBG 1 inscribed by the femtosecond laser at 520 nm.

The TFBG inscription system is sketched in Fig. 1. The femtosecond laser (SpOne-8-SHG, Newport) emits pulses at 520 nm with a pulse duration of 346 fs and a maximal repetition rate of 200 kHz. The fiber sample was immobilized on a multi-axis tilt platform (M-37, Newport) integrated on a three-axis precision translation stage (X/Y: XMS100-S, Z: M-VP-5ZA, Newport). An oil-immersion objective (60×, NA = 1.42, UPLXAPO60XO, Olympus) was used to focus the beam onto the fiber core. More information related to this inscription system can be found in Ref. [16]. Prior to TFBG inscription, the POFs were pre-annealed at 130°C for two days for the release of frozen-in stress generated during the fiber drawing process [33]. Then, both ends of the POFs (~4 cm in length) were spliced to silica fiber pigtails by a UV-glue (Norland 86 H) method in order to monitor the reflected and transmitted spectra during the grating photo-inscription process.

A diagram of the laser-scanning process is shown in Fig. 2(a). Each grating line (white color) has a length of 10 μm and a tilt angle of 8°. The laser pulse energy, repetition rate, and scanning speed were 6.0 nJ, 1000 Hz, and 250 μm/s, respectively. The LbL inscription was repeated 3000 times with a grating period of 1.0446 μm, so that a 3.1-mm-long TFBG (labeled TFBG 1 in the following) was obtained. A microscope image of this TFBG is presented in Fig. 2(b), clearly showing refractive index modifications induced by the femtosecond laser. Both the reflected and transmitted spectra were monitored by an FBG interrogator (FS22SI, HBM Fiber Sensing) featuring a wavelength resolution of 1 pm and a scanning rate of 1 Hz.

Figure 3 shows both the reflected and transmitted amplitude spectra after inscription compared to the original transmitted spectrum of the fiber before the inscription of TFBG 1. The fundamental core mode resonance at ~1573 nm appears in both reflected and transmitted spectra. Several tens of cladding

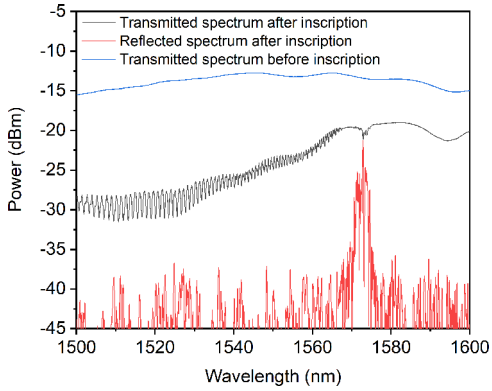

Fig. 3. Reflected and transmitted spectra after inscription compared to the original transmitted spectrum before inscription of the 3.1-mm-long 8° TFBG (TFBG 1).

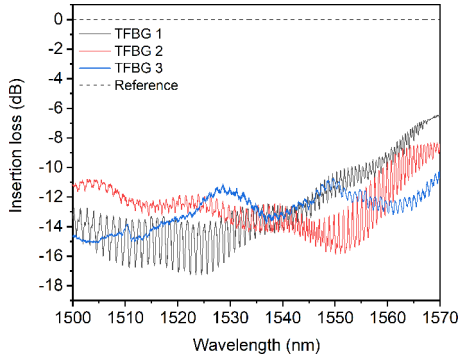

Fig. 4. Normalized transmitted spectra with respect to the original spectra before the inscription of three TFBGs featuring the same tilt angle but different writing parameters.

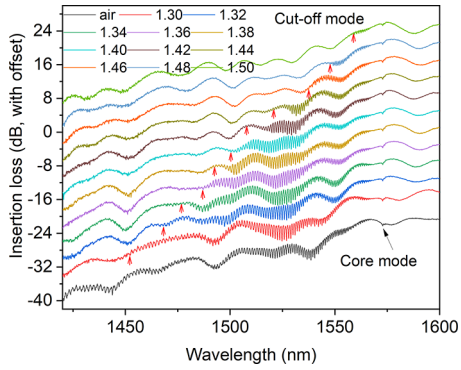

Fig. 5. Transmitted spectrum evolution (vertical scale with offset) as a function of the SRI in the range 1.30–1.50 for the 3.1-mm-long 8° TFBG (TFBG 1).

mode resonances could be found at wavelengths smaller than ~1568 nm. According to the TFBG phase-matching principle, each cladding mode resonance features a unique effective refractive index [17,18]. The FWHM (full width at half maximum) of a resonance is ~400 pm and the interval between two adjacent resonances is typically in the range of 0.5–1.5 nm. However, compared with the initial spectrum before inscription, the out-of-band insertion loss (OBIL) of the core mode in the transmitted spectrum is ~6 dB, while the counterpart for the cladding mode is even higher: ~13 dB. The OBIL could result from the propagation light scattering due to the inhomogeneity of the refractive index modulation in the fiber induced by the femtosecond laser direct writing process [30]. Although these values are larger than what are usually induced in silica optical fibers, it does not affect the SRI sensing capability, as demonstrated in the following.

Two other TFBGs (2 and 3) were inscribed with different parameters for comparison. The data are shown in Table 1. The normalized transmitted spectra with respect to the fiber transmission before inscription are shown in Fig. 4.

Compared to TFBG 1, TFBG 2 was produced at a higher scanning rate and contains more grating periods, inducing a similar cladding mode amplitude and OBIL. It is worth mentioning that the cladding mode amplitude appears with the OBIL. Thus, a trade-off between them could be considered regarding TFBG fabrication in this type of fiber. TFBG 3 was inscribed with a higher pulse energy and fewer periods compared to TFBG 2. Consequently, smaller cladding mode amplitudes and a similar OBIL were obtained.

TFBG 1 was characterized for refractometric measurements. The evolution of the transmitted spectrum was measured by immersing the TFBG successively in calibrated liquids (Cargille oils) with refractive indices ranging from 1.30 to 1.50 in intervals of 0.02. A supercontinuum light source (SC-5-FC, YSL Photonics) was used, and measurements were recorded in the range of 1420–1600 nm by an optical spectrum analyzer (MS9740A, Anritsu). The transmitted amplitude spectrum evolution as a function of the SRI is shown in Fig. 5. The red and black arrows in the figure indicate the cutoff modes of the cladding mode resonances and the core mode, respectively.

It can be seen that for the transmitted amplitude spectrum measured in air, the cladding mode resonances extend to ~1420 nm on the left, so they can span a large spectral range of 147 nm. Considering the phase-matching conditions of TFBGs, this cladding mode expansion confirms the potential to measure SRIs slightly lower than 1.30. Hence, when increasing the SRI values from 1.30 to 1.50, the cladding mode resonances gradually disappear from the left to the right of the spectral range. This behavior arises from the fact that when the SRI reaches the effective refractive index of a cladding mode, the latter is no longer reflected at the interface between the cladding and the surroundings and is radiated into the surrounding medium. The refractometric sensing range is much larger than those for TFBGs in PMMA POFs [25,26].

From the raw data displayed in Fig. 5, the refractometric sensitivity of the 8° TFBG was calculated following two methodologies. The first one is the most sensitive and consists in tracking the wavelength shift of the cutoff cladding mode resonance, i.e.,

Table 1. Data for TFBGs Inscribed by the Femtosecond Laser

TF BG	Scanning Rate (μm/s)	Repetition Rate (Hz)	Pulse Energy (nJ)	Grating Period (μm)	Number of Periods	Cladding Mode Amplitude (dB)	OBIL of Cladding Modes (dB)
1	250	1000	6.0	1.0446	3000	~3	~13
2	300	1000	6.0	1.0514	4000	~3	~13
3	300	1000	6.1	1.0545	3000	~1	~12

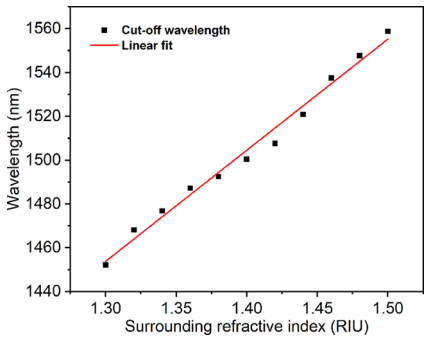

Fig. 6. Evolution of the cutoff cladding mode in the transmitted spectrum as a function of the SRI for TFBG 1.

the one for which the effective refractive index is slightly above the SRI value. This evolution is shown in Fig. 6. Following a linear regression of the raw data, a refractometric sensitivity of 507 nm/RIU was obtained. The R^2 was computed to be 98.7%, which confirms the good linearity of the response. The sensitivity for the cutoff mode is comparable to the counterpart for the TFBG in the silica fiber [24].

The evolutions of selected cladding mode resonances near the cutoff wavelength were also tracked. It turns out that the sensitivity is at least 6 nm/RIU at different wavelengths, such as ~1515 nm, ~1539 nm, and ~1561 nm. This decrease in sensitivity was expected but confirms that different modes can be tracked for a reliable demodulation process.

In this Letter, we have reported the first inscriptions of TFBGs in single-mode step-index TOPAS/ZEONEX POFs based on a 520 nm femtosecond laser and the LbL inscription technique. The fiber materials and the chosen tilt angle of 8° allow the excitation of cladding mode resonances in a large spectral range of 147 nm, which enables effective refractive index sensitivity in aqueous solutions. The evolution of the transmitted amplitude spectrum was analyzed as a function of SRI from 1.30 to 1.50. Spectral shifts of the cutoff cladding mode showed a sensitivity of 507 nm/RIU. For individual cladding mode resonances, their spectral shifts yielded sensitivities of at least 6 nm/RIU. The breakthrough of achieving a large refractive index sensing range including aqueous solutions paves the way to the future application of POF-TFBG in (bio)chemical sensing. TFBGs with unique POF advantages can be potentially used as wearable sensors in healthcare fields for multi-parameter measurements, such as those of human physiological signs, body functionalities, pH, sodium chloride concentration, etc.

Funding. Special Projects in Key Fields of Colleges and Universities in Guangdong Province (2020ZDZX3037); Science and Technology Department of Guangdong Province (2022A1515012571); Fonds De La Recherche Scientifique - FNRS.

Acknowledgments. Funding from Fonds de la Recherche Scientifique (F.R.S.-FNRS) is under the Postdoctoral Researcher grant (Chargé de Recherches) of Xuehao Hu and the Senior Research Associate Position of Christophe Caucheteur

Disclosures. The authors declare no conflicts of interest.

Data availability. Data underlying the results presented in this paper are not publicly available at this time but may be obtained from the authors upon reasonable request.

REFERENCES

1. Z. Xiong, G. D. Peng, B. Wu, and P. L. Chu, IEEE Photonics Technol. Lett. **11**, 352 (1999).
2. H. Dobb, D. J. Webb, K. Kalli, A. Argyros, M. C. J. Large, and M. A. van Eijkelenborg, Opt. Lett. **30**, 3296 (2005).
3. J. Bonefacino, H.-Y. Tam, T.-S. Glen, X. Cheng, C. F. J. Pun, J. Wang, P.-H. Lee, M. L. V. Tse, and S.-T. Boles, Light: Sci. Appl. **7**, 17161 (2018).
4. I. P. Johnson, W. Yuan, A. Stefani, K. Nielsen, H. K. Rasmussen, L. Khan, D. J. Webb, K. Kalli, and O. Bang, Electron. Lett. **47**, 271 (2011).
5. W. Yuan, L. Khan, D. J. Webb, K. Kalli, H. K. Rasmussen, A. Stefani, and O. Bang, Opt. Express **19**, 19731 (2011).
6. C. Markos, A. Stefani, K. Nielsen, H. K. Rasmussen, W. Yuan, and O. Bang, Opt. Express **21**, 4758 (2013).
7. A. Leal-Junior, A. Theodosiou, C. Díaz, C. Marques, M.-J. Pontes, K. Kalli, and A. Frizera-Neto, Polymers **10**, 674 (2018).
8. G. Woyessa, A. Fasano, C. Markos, A. Stefani, H. K. Rasmussen, and O. Bang, Opt. Mater. Express **7**, 286 (2017).
9. J. N. Dash, X. Cheng, D. S. Gunawardena, and H.-Y. Tam, Photonics Res. **9**, 1931 (2021).
10. G. Woyessa, A. Fasano, C. Markos, H. K. Rasmussen, and O. Bang, IEEE Photonics Technol. Lett. **29**, 575 (2017).
11. W. Zhang and D. Webb, Opt. Lett. **39**, 3026 (2014).
12. H. Y. Liu, G. D. Peng, and P. L. Chu, IEEE Photonics Technol. Lett. **14**, 935 (2002).
13. X. Hu, G. Woyessa, D. Kinet, J. Janting, K. Nielsen, O. Bang, and C. Caucheteur, Opt. Lett. **42**, 2209 (2017).
14. L. Pereira, R. Min, X. Hu, C. Caucheteur, O. Bang, B. Ortega, C. Marques, P. Antunes, and J. L. Pinto, Opt. Express **26**, 18096 (2018).
15. A. Theodosiou and K. Kalli, Opt. Fiber Technol. **54**, 102079 (2020).
16. X. Hu, Z. Chen, X. Cheng, R. Min, H. Qu, C. Caucheteur, and H.-Y. Tam, Opt. Lett. **47**, 249 (2022).
17. T. Guo, F. Liu, B.-O. Guan, and J. Albert, Opt. Laser Technol. **78**, 19 (2016).
18. J. Albert, L.-Y. Shao, and C. Caucheteur, Laser Photonics Rev. **7**, 83 (2013).
19. K. A. Konnov, S. V. Varzhel, and A. I. Gribaev, Opt. Quantum Electron. **52**, 169 (2020).
20. A. Ioannou, A. Theodosiou, C. Caucheteur, and K. Kalli, Opt. Lett. **42**, 5198 (2017).
21. K. Zhou, A. G. Simpson, L. Zhang, and I. Bennion, IEEE Photonics Technol. Lett. **15**, 936 (2003).
22. C. Caucheteur, T. Guo, and F. Liu, Nat. Commun. **7**, 13371 (2016).
23. A. Ioannou, A. Theodosiou, K. Kalli, and C. Caucheteur, Opt. Lett. **43**, 2169 (2018).
24. X. Hu, Y. Liu, J. Jiang, W. Lin, H. Qu, and C. Caucheteur, IEEE Sens. J. **22**, 2229 (2022).
25. X. Hu, C. Pun, H. Tam, P. Mégret, and C. Caucheteur, Opt. Lett. **39**, 6835 (2014).
26. X. Hu, P. Mégret, and C. Caucheteur, Opt. Lett. **40**, 3998 (2015).
27. T. Erdogan and J. E. Sipe, J. Opt. Soc. Am. A **13**, 296 (1996).
28. G. Woyessa, A. Fasano, A. Stefani, C. Markos, K. Nielsen, H. K. Rasmussen, and O. Bang, Opt. Express **24**, 1253 (2016).
29. C. E. Porter and F. D. Blum, Macromolecules **33**, 7016 (2000).
30. J. He, B. Xu, X. Xu, C. Liao, and Y. Wang, Photonics Sens. **11**, 203 (2021).
31. X. Hu, Y. Chen, S. Gao, R. Min, G. Woyessa, O. Bang, H. Qu, H. Wang, and C. Caucheteur, Polymers **14**, 1350 (2022).
32. D. J. Webb, Meas. Sci. Technol. **26**, 092004 (2015).
33. W. Yuan, A. Stefani, M. Bache, T. Jacobsen, B. Rose, N. Herholdt-Rasmussen, F. K. Nielsen, S. Andresen, O. B. Sørensen, K. S. Hansen, and O. Bang, Opt. Commun. **284**, 176 (2011).